IEEE Access
Multidisciplinary | Rapid Review | Open Access Journal

Received May 30, 2019, accepted June 20, 2019, date of publication June 26, 2019, date of current version July 16, 2019.

Digital Object Identifier 10.1109/ACCESS.2019.2925182

Adaptive Trajectory Tracking Control of a Parallel Ankle Rehabilitation Robot With Joint-Space Force Distribution

MINGMING ZHANG[1], (Member, IEEE), ANDREW MCDAID[2], (Member, IEEE), ALLAN J. VEALE[3], YUXIN PENG[4], AND SHENG QUAN XIE[5], (Senior Member, IEEE)

[1]Department of Biomedical Engineering, Southern University of Science and Technology, Shenzhen 518055, China
[2]Department of Mechanical Engineering, The University of Auckland, Auckland 1010, New Zealand
[3]Department of Biomechanical Engineering, University of Twente, 7522 Enschede, The Netherlands
[4]Department of Physical Education and Sports Science, Zhejiang University, Hangzhou 310028, China
[5]School of Electronic and Electrical Engineering, University of Leeds, Leeds LS2 9JT, U.K.

Corresponding author: Mingming Zhang (zhangmm@sustech.edu.cn)

This work was supported by The University of Auckland through the Faculty of Engineering Research Development Fund (Physical Robot-Human Interaction for Performance-Based Progressive Robot-Assisted Therapy) under Grant 3625057.

ABSTRACT This paper proposes an adaptive trajectory tracking control strategy implemented on a parallel ankle rehabilitation robot with joint-space force distribution. This device is redundantly actuated by four pneumatic muscles (PMs) with three rotational degrees of freedom. Accurate trajectory tracking is achieved through a cascade controller with the position feedback in task space and force feedback in joint space, which enhances training safety by controlling each PM to be in tension in an appropriate level. At a high level, an adaptive algorithm is proposed to enable movement intention-directed trajectory adaptation. This can further help to improve training safety and encourage human–robot engagement. The pilot tests were conducted with an injured human ankle. The statistical data show that normalized root mean square deviation (NRMSD) values of trajectory tracking are all less than 2.3% and the PM force tracking being always controlled in tension, demonstrating its potential in assisting ankle therapy.

INDEX TERMS Parallel ankle robot, movement intention, cascade control, trajectory adaptation, force distribution.

I. INTRODUCTION

Robot-assisted rehabilitation solutions have been actively researched in the past few decades [1]–[3]. A systematic review of 29 studies with a total of 164 patients and 24 healthy subjects demonstrates the effectiveness of existing rehabilitation robots in reducing ankle impairments [4]. With respect to wearable robotic exoskeletons that aim more at gait assist [5], [6] and single-degree of freedom (DOF) ankle rehabilitation devices [7], parallel mechanisms are better suited for ankle exercises in a three-dimensional space due to the characteristics of multiple DOFs, safe workspace and large actuation torque [4].

A variety of parallel robotic platforms have been developed for ankle therapy. The Rutgers Ankle is powered by double-acting pneumatic cylinders [8]. While its effectiveness has been validated on subjects with varying grades of ankle sprains [9], stroke patients [10], and children with cerebral palsy [11], it has difficulties in predefining training paths due to its misaligned rotation center with human ankles or aligned rotation center at the expense of limited workspace. Saglia, *et al.* [12] used a strut with three linear electric actuators in a parallel ankle device, with a similar issue of a misaligned rotation center with the Saglia, *et al.* [13]. Some other parallel mechanisms have been also developed for ankle therapy [14]–[16], but few have integrated the features of multiple DOFs, aligned rotation center with human ankle, and adaptive trajectory adaptation.

To ensure aligned rotation centers of the robot and the human ankle, Tsoi, *et al.* [17] replaced the middle strut with human lower limbs. While this matches anatomical ankle by placing four actuators above the end effector,

The associate editor coordinating the review of this manuscript and approving it for publication was Yongping Pan.

unexpected loads can be exerted and may even cause injuries. To avoid using human limbs as constrains, Jamwal, *et al.* [18] developed a three-DOF robotic device by setting physical rotation axes for the moving platform. While this device was designed with intrinsic compliance by using pneumatic muscles (PMs, Shadow Air Muscles), it suffers from the issue of limited actuation torque at extreme PM contraction. It has not been implemented with interactive training strategies due to the lack of built-in sensors for measuring real-time human-robot interaction. Jamwal, et just achieved trajectory tracking by controlling each PM length in joint space. The structural evolution of ankle robots has been also presented in [19].

Zhang, *et al.* [20] further improved this robotic system by using Festo fluidic muscles, integrating a six-axis load cell and three rotary sensors. While the implementation of an adaptive admittance control enhances safe human-robot interaction, this scheme does not fundamentally address the low-level issue of no joint-space force control. On cable-driven devices, however, this may cause safety issues if some actuators become loose [21], [22]. Another concern is that the robot workspace can be limited if PMs are not controlled with minimum energy consumption, based on a fact that PMs' displacement and load are in an inverse relationship at a certain pressure.

This study proposes a new control strategy to solve the safety issues as presented in [18], [20], and also to ensure an optimal robot workspace. It is implemented through a cascade controller with posture control in task space and individual actuator force control in joint space. Further, a high-level trajectory adaptation algorithm is proposed for movement intention-directed training. This helps to enhance the training safety by avoiding excessive interaction force, and also verify the cascade controller.

II. ROBOT DESCRIPTION AND ANALYSIS

The ankle robot is presented in FIGURE 1, as well as its control box. The robot development has been reported in our previous works [23], [24]. It has three rotational DOFs that are actuated by four PMs (Festo DMSP-20-400N, Germany) in parallel. These DOFs are for ankle dorsiflexion/plantarflexion (DP), inversion/eversion (IE) and internal/external rotation (IER), respectively. Their corresponding angular positions are denoted as $\theta_x, \theta_y, \theta_z$, and similarly trajectories as X, Y, Z. The sensing components include three magnetic rotary encoders (AMS AS5048A, Austria) for measuring angular positions of the footplate, four single-axis load cells (Futek LCM 300, United States) for measuring actuator contraction force, and four proportional pressure regulators (Festo VPPM-6L-L-1-G18-0L6H, Germany), for the pressure control of the PMs. The six-axis load cell (SRI M3715C, China) is installed between the footplate and the link 3 of the moving platform for measuring human-robot interaction. All electronic components communicate with the embedded controller (NI Compact RIO-9022, United States) through three modules for digital input/output (NI 9401), analog input (NI 9205), analog output (NI 9263), and the RS 232 port.

To achieve accurate control of the parallel ankle robot, the following information is required, involving PM modeling, robot kinematics/dynamics, and force distribution from task space torque to joint space force. While this has been reported in [23], a brief description of the method is still presented here to facilitate readers' understanding.

A. PM MODELING

PMs are highly nonlinear which requires accurate modeling for control. In this study, a forward control is used based on the PM model of Sarosi [25]. The model is represented in (1), where muscle strain $k = (l_0 - l)/l_0$, F the muscle contraction force, p the measured muscle pressure, l_0 the initial muscle length, l the actual muscle length. Other parameters a, b, c, d, e were experimentally obtained and given in [25].

$$F(p, k) = (p + a)\, e^{bk} + cpk + dp + e \tag{1}$$

B. ROBOT KINEMATICS AND DYNAMICS

The ankle robot has three rotational DOFs based on a parallel mechanism. The posture $(\theta_x, \theta_y, \theta_z)$ of the footplate can be measured from three built-in magnetic rotary encoders. Further to use inverse kinematics of parallel mechanisms, the required link length can be uniquely determined for a specific posture.

Knowledge of the inertial properties of the moving platform is also crucial to robot motion control. The mass, center of mass and inertia tensor of each link can be obtained from the Creo model. Thus, the global inertial tensor and gravitational effect of the moving platform is derived, as well as the robot dynamics equation, where the human-robot interaction is measured through the six-axis load cell and the friction part is ignored for simplification. More details are reported in [23].

C. FORCE DISTRIBUTION

Cable-driven robots may lose controllability if certain cables are not in tension during the robotic operation [21]. The ankle robot employs PMs that work similar to cables along actuators, and thus it is necessary to control individual actuator force to ensure safety. This requires conducting force distribution from required robot torque T_r to required individual actuator force F_i.

An analytic-iterative force distribution technique can be well implemented with the ankle robot [26]. The method is formulated into an optimization problem (2),

$$\begin{cases} min\, f\,(y) = (F_o + By)^T (F_o + By) \\ \text{Subject to } F_{min} - (F_o + By) \le 0 \end{cases} \tag{2}$$

where $B = I - A^+ A$, and then handled by the Karush–Kuhn–Tucker theorem. This approach uses a search algorithm, and thus the absolute sum of link forces is smaller than that of the closed-form method [27]. This means that using the analytic-iterative method the robot can achieve required

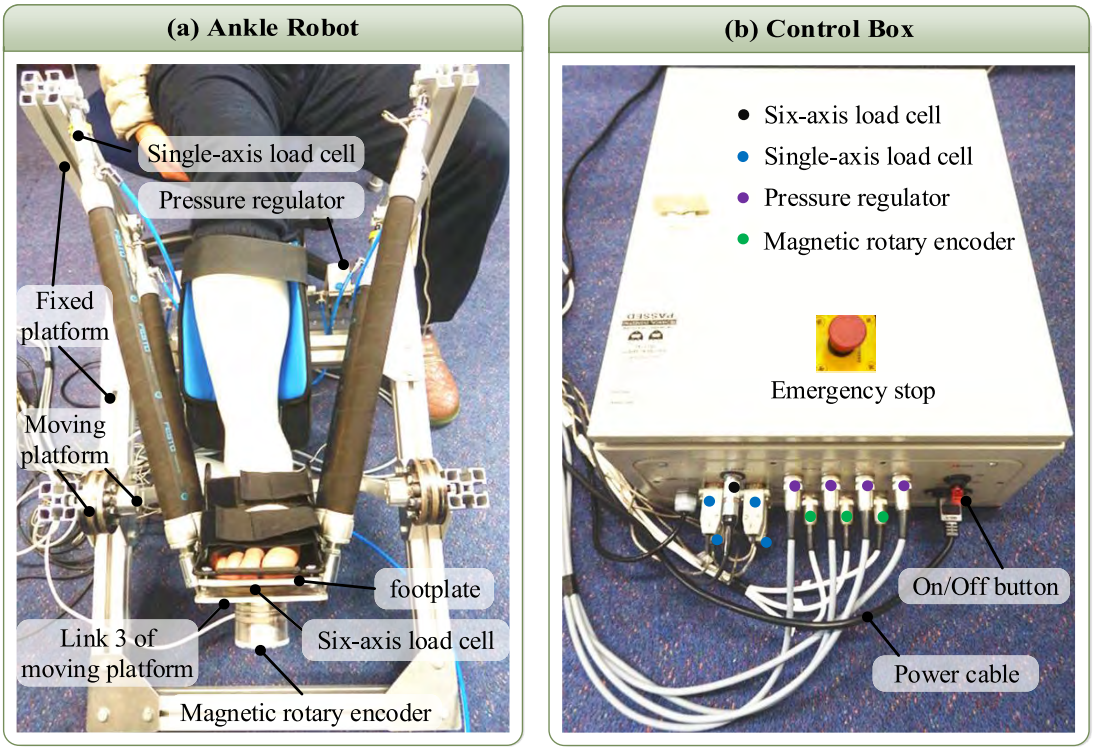

FIGURE 1. The ankle robot (a) and control box (b).

movement with less energy consumption under same external load.

Noting that the consumed time for one sample of force distribution in MATLAB simulation is less than 0.0005s, while the ankle robot operates with the bandwidth of 0.02s. That is, this method can meet the requirement of real-time control for rehabilitation training on the robotic system.

III. CONTROL SYSTEM

The ankle robot is implemented with a low-level cascade controller for trajectory tracking. In the high level, a movement intention-directed control strategy is proposed by allowing real-time trajectory adaptation based on human-robot interaction, as presented in FIGURE 2.

A. CASCADE CONTROL WITH JOINT-SPACE FORCE DISTRIBUTION

Trajectory tracking by only controlling PM length cannot guarantee all PMs in tension, which may be unsafe for human users [18], [21], [22]. As in FIGURE 2, the proposed cascade controller measures orientation of the footplate as feedback in the outer loop, and PM forces as feedback in the inner loop. This guarantees not only trajectory tracking accuracy, but also ensure the PMs always in tension for training safety. An analytic-iterative technique [26] is used for force distribution. This helps to optimize the robot workspace when meeting a specific torque requirement. Specifically, this is a redundant robotic system so that there can have a number of solutions (different combinations of the four actuator forces) for a given robotic torque. Further to consider PMs' characteristics, an optimization-based force distribution method can be used to determine a minimum force consumption of the actuators, and thus larger actuator stroke and optimal robot workspace.

B. ADAPTIVE TRAJECTORY TRACKING CONTROL

An adaptive control strategy was proposed for movement intention-directed training. Human users can achieve self-initiated movements by allowing adaptation of training trajectories when a force or torque threshold is triggered by the participant's ankle. In this study, the interaction force is used to trigger trajectory adaptation. This is because users' movement intention is more sensitive to interaction force than torque with the current training protocol based on pilot tests. The force threshold will be determined according to human users' force ability and be set under the supervision and experience of a therapist. A sinusoidal training path is selected as the reference trajectory since it mirrors the principle of manual physiotherapy with continuously changing position and speed, and its movement status can be adjusted through the phase and frequency.

To make trajectory adaptation clear, a brief description of the algorithm is given first. The initial reference trajectory x_{init} is defined in (3), where A_x is the amplitude, f is the frequency, and t is the time. If an interaction force F_x along ankle DP is exerted and reaches a predefined threshold F_{0x}, a modified trajectory $x_{adap}(t)$ is generated as in (4), when the time is taken as t_1, the displacement as x_1, the velocity as $x_1^{'}$,

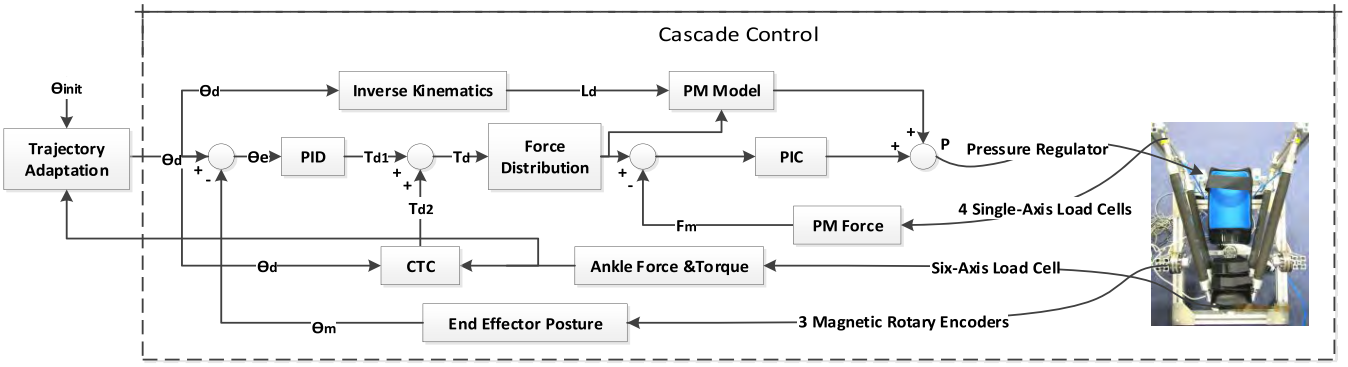

FIGURE 2. A cascade controller (in a dashed line frame) with position control in outer loop and PM force control in inner loop. CTC: Computed torque controller; PID: Proportional-integral-derivative; PIC: Proportional-integral controller; PM modeling relates to Equation (1); Force distribution refers to Equation (2) for the analytic-iterative method; the position tracking error is denoted by θ_e, $\theta_e = \theta_d - \theta_m$, of which θ_d represents the desired position of the end effector while θ_m represents the measured position; T_d represents the desired torque; F_m represents the measured contraction force of the PM; L_d and V_d represents the desired PM length and its velocity; and P represents the PM pressure.

and the modified phase φ_{xadap} is given in (5).

$$x_{init}(t) = A_x \sin(2\pi f t) \tag{3}$$

$$x_{adap}(t) = x_{init}\left(t + \varphi_{xadap}\right) \tag{4}$$

$$\varphi_{xadap} = \begin{cases} \dfrac{1}{2f} - \dfrac{arcsin(|x_1|/A_x)}{\pi f}, \\ \qquad if\ x_1 \geq 0,\ x_1^{'} \geq 0,\ F_x < -F_{0x} \\ -\dfrac{1}{2f} + \dfrac{arcsin(|x_1|/A_x)}{\pi f}, \\ \qquad if\ x_1 \geq 0\,,x_1^{'} < 0,\ F_x \geq F_{0x} \\ \dfrac{1}{2f} - \dfrac{arcsin(|x_1|/A_x)}{\pi f}, \\ \qquad if\ x_1 < 0,\ x_1^{'} < 0,\ F_x \geq F_{0x} \\ -\dfrac{1}{2f} + \dfrac{arcsin(|x_1|/A_x)}{\pi f}, \\ \qquad if\ x_1 < 0,\ x_1^{'} \geq 0,\ F_x < -F_{0x} \end{cases} \tag{5}$$

wo cases are defined to describe the trajectory adaptation algorithm. Case 1 is consistent interaction force direction as the current training path, where human-robot interaction torque does not redirect the robotic movement. Case 2 is an interaction force to resist the robot movement, where a new trajectory is generated following the rule of (4, 5) to fit participants' movement intention. The robot continues to move towards the zero-crossing point. The resulting time is taken as t_2 when the robot reaches the zero-crossing point, as in (6), and the value A_x is set zero. To continue, the participant initiates a new training trajectory laterally (along ankle IE), when the time is taken as t_3. This route can be initiated when an interaction force F_y triggers the force threshold F_{0y}, as in (7, 8). The modified phase φ_{yadap} is obtained using the same method as φ_{xadap}. By this algorithm, the robot can initiate training based on the patient's movement intention in one direction, or switch trajectories for different directions at the zero-crossing point.

$$t = t_2, when\ x_{adap}(t) = 0 \tag{6}$$

$$y_{adap}\left(t_y\right) = A_y \sin\left(2\pi f\left(t_y + \varphi_y + \varphi_{yadap}\right)\right) \tag{7}$$

$$t_y = t - t_3, \varphi_y = \begin{cases} 0, & if\ F_y \geq F_{0y} \\ 1/2f, & if\ F_y < -F_{0y} \end{cases} \tag{8}$$

The robot movement speed can be also adapted when continuous interaction forces reach the predefined threshold. Take the initial trajectory (3) for instance, the frequency f can be adaptively modified to f_{adap}, as in (9), where f_0 is the initial frequency, and k_f is a coefficient that reflects the influence of human users.

$$f_{adap} = (F - F_0)/k_f I + f_0 \tag{9}$$

To better explain the movement intention-directed trajectory adaptation method, a simulation was conducted in MATLAB, as presented in FIGURE 3. It can be seen that the proposed algorithm is able to modify the reference trajectory in a way desired by the patient. For example, at 2s an interaction force F_x triggers the threshold F_{0x}, the trajectory reverses by moving the phase by $1/2f - arcsin(|x_1|/A_x)/\pi f$. During 20-30s, the resisting force is applied at T_1, the trajectory X is controlled to reach zero-crossing point at T_2, and the transition between trajectories X and Y is completed at T_3, as labelled in FIGURE 3, when an interaction force F_y triggers the threshold F_{0y}.

IV. EXPERIMENTS AND RESULTS

This robot can be reconfigured to achieve varying workspace and torque actuation capacity, and its kinematic configuration used in this study is reported in [24]. Such a configuration does not allow independent control of ankle IER. Experiments were conducted with the approval by the University of Auckland, Human Participants Ethics Committee (011904).

A. TRAJECTORY TRACKING WITH FORCE DISTRIBUTION

The training using the cascade controller was conducted on a subject (male, 29 years, two months after ankle sprain). On the experiment day, the ankle joint was diagnosed as limited ranges of motion (ROMs) and strength, one week after

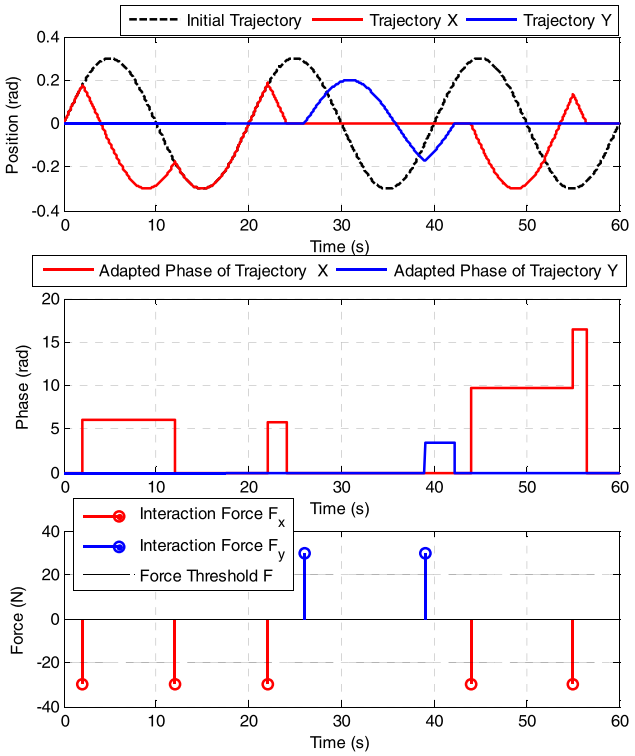

FIGURE 3. Simulation of the proposed trajectory adaptation algorithm. (The bottom plot shows measured human-robot interaction forces. These forces cause phase adaptation as in middle plot, leading to trajectory adaptation, as in the top plot.).

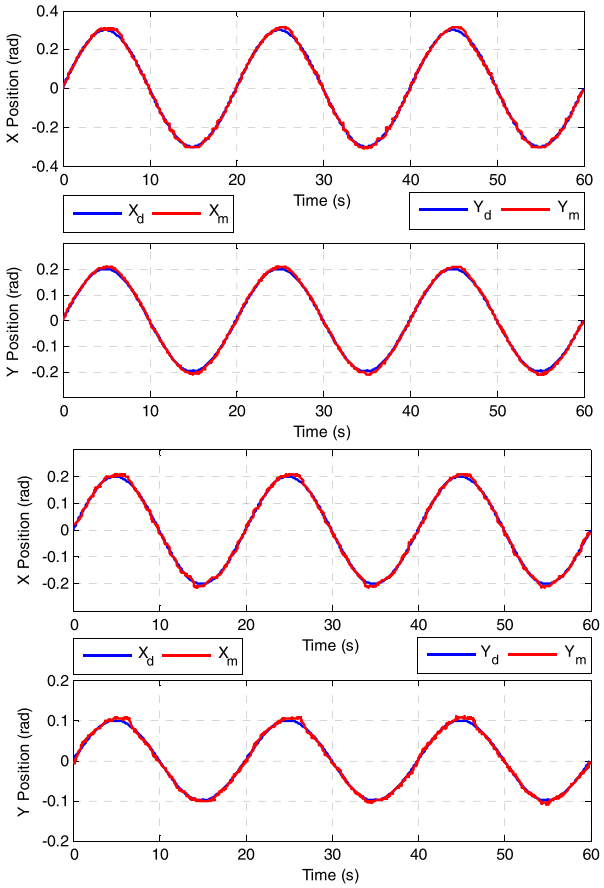

FIGURE 4. Trajectory tracking responses of the single-axis training (top two) and the mixed-axis training (bottom two). X refers to ankle DP, and Y for ankle IE.

ankle sprain. Before the training, a preliminary assessment was conducted to check the appropriate ankle ROMs, and a physical therapist recommended training of only ankle DP and IE at this stage. It was suggested that the amplitudes of the single-axis training for ankle DP and IE are 0.3 rad and 0.2 rad, respectively, and for mixed-axis training 0.2 rad for ankle DP and 0.1 rad for ankle IE. The subject was then instructed to sit on a height-adjustable chair with the shank free on the leg holder. The foot was strapped into the ankle orthosis. All predefined trajectories were set to operate three cycles with 0.05 Hz. The participant was asked to remain relaxed during the training. Preliminary results are presented in Figs. 4 and 5. FIGURE 4 plots the trajectory tracking responses of the single-axis training and the mixed-axis training. FIGURE 5 presents the individual PM force tracking responses of the single-axis and mixed-axis training. It should be noted that the minimum force was set at zero for force distribution.

Statistical results of the tracking accuracy are summarized in TABLE 1 at the end of Section IV. It can be seen from the table that the trajectory tracking performance is pretty good, with all the normalized root mean square deviation (NRMSD) values no more than 2.21%. In joint space, while the NRMSD values of force tracking range from 7.62% to 20.24%, it is obvious in FIGURE 5 that all PMs' forces are controlled at above zero. This is extremely important to cable-driven robotic devices.

B. ADAPTIVE TRAJECTORY TRACKING CONTROL

The participant also conducted adaptive training based on his movement intention. The amplitude of the initial trajectory is 0.3 rad for ankle DP and 0.2 rad for ankle IE, also with the frequency of 0.05 Hz. The force or torque threshold was set at 20 N based on the ability of the patient under the supervision of a therapist. Preliminary results on the ankle robot system are presented in Figs. 6 and 7. In FIGURE 6, the top and middle plots are the desired and measured trajectory of X and Y, respectively, and the bottom is the force trigger events. It is clear that the trajectory adaptation control law could direct the robot movement keeping consistent with the patient's intended force. The robot was controlled using the proposed trajectory adaptation algorithm: training along X during 0-44s, along Y during 49-63, and back along X during 65-90s. Further, this algorithm allows for adaptive frequency adaptation of the trajectory, as indicated in Equations (3-4), which has been demonstrated in FIGURE 6 during the periods of 73-76s and 84-86s.

FIGURE 7 presents individual actuator force tracking of the ankle robot under the mode of movement intention-directed training. It can be seen from TABLE 1 that the NRMSD values of force tracking range from 8.48% to 14.5%,

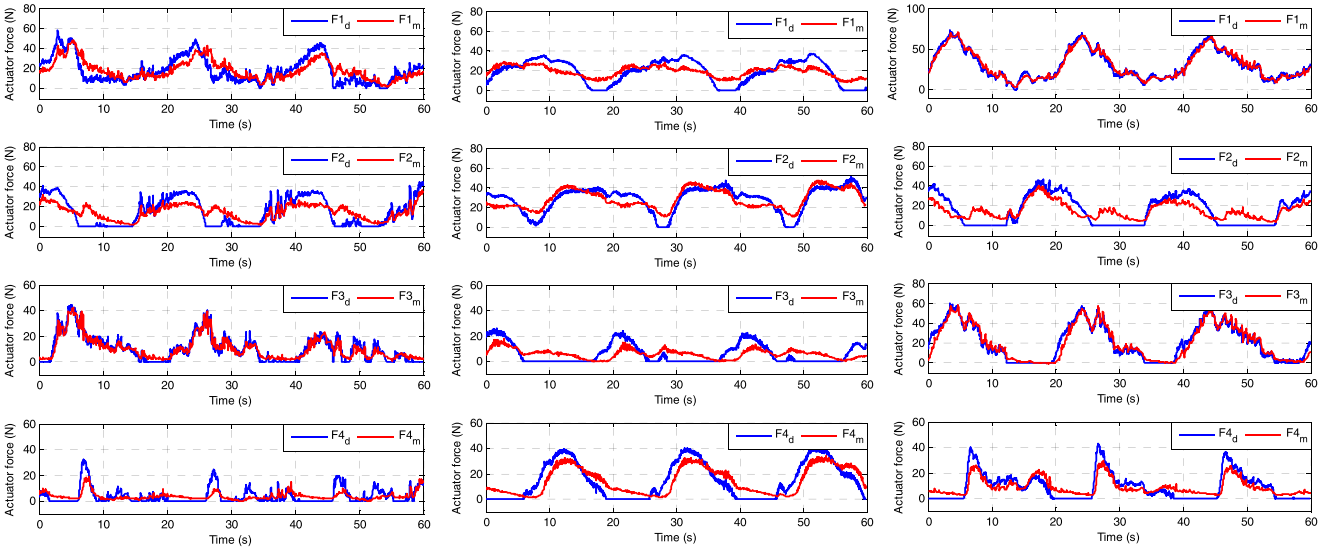

FIGURE 5. Individual PM force tracking responses of the single-axis ankle DP (left) and IE (middle) training, and the mixed-axis training (right). The subscript d and m represent desired and measured, respectively.

TABLE 1. Statistical results of the controlled variables of the robot.

		Single-Axis		Mixed-Axis	Adaptive Training
		X	Y	XY	
F1 (N)	RMSD	7.8704	8.0096	3.1579	8.4771
	NRMSD	13.51%	21.47%	4.35%	11.44%
F2 (N)	RMSD	9.2379	7.3678	9.2175	9.0588
	NRMSD	20.24%	14.62%	20.1%	14.13%
F3 (N)	RMSD	3.3823	6.8512	4.6860	5.0518
	NRMSD	7.62%	26.5%	7.88%	8.48%
F4 (N)	RMSD	4.6678	7.6453	5.7107	5.5659
	NRMSD	14.37%	19.03%	13.4%	14.5%
X (rad)	RMSD	0.0083	—	0.0061	0.0124
	NRMSD	1.39%	—	1.53%	2.07%
Y (rad)	RMSD	—	0.0053	0.0044	0.0064
	NRMSD	—	1.32%	2.21%	2.08%

RMSD: Root mean square deviation; NRMSD: Normalized root mean square deviation; — represents not applicable.

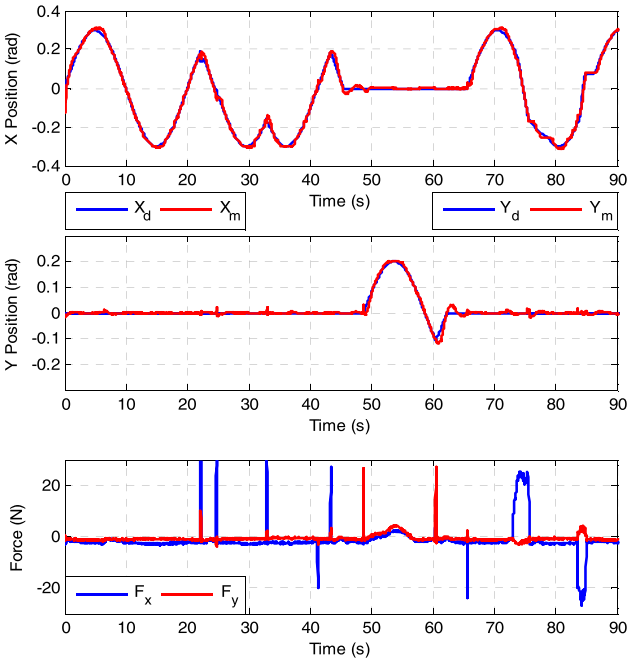

FIGURE 6. Trajectory tracking responses of the adaptive training. Starting from ankle DP until around the 44th s, then change to ankle IE from the 49th to 63th s, and finally back to ankle DP from the 65th s.

and those of trajectory tracking are 2.07% and 2.08%, respectively. While some saltation points of the measured PM force exist, this is caused by the saltatorial desired force. Further, it is caused by sudden patient-robot interaction, and can be easily filtered out. Generally, if the patient does not intend to change the robot movement, or is severely impaired without enough muscle force, the robot will operate in a passive mode by tracking a predefined trajectory. If the patient tries to actively participate and interact with force above the predefined threshold, the robot switches to an active mode in which trajectory parameters can be recalculated.

By comparing tracking responses of different training modes, as summarized in TABLE 1, it was found that the trajectory tracking accuracy of the single-axis training presents better than those of the mixed-axis training and the adaptive training, with the NRMSD values of the single-axis training less than 1.4%, while the other NRMSD values being around 2%, which is reasonable since more uncertainties were brought in for the mixed-axis and the movement intention-directed training. Note that while the proposed control method shows great potential, this cannot prove which training mode performs best due to small samples of data.

Further in TABLE 1, most NRMSD values of PMs' force tracking are greater than those of the trajectory tracking. Accurate force control is really difficult to be achieved especially under the presence of human-robot interaction.

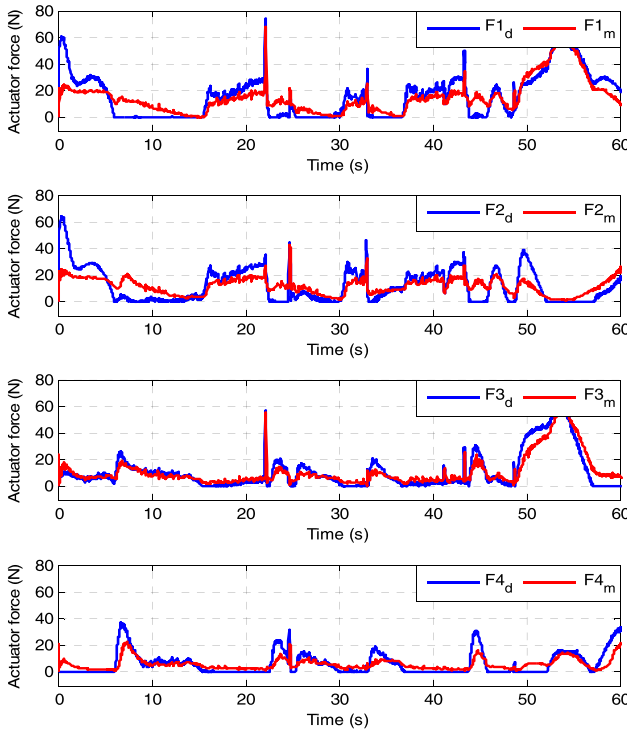

FIGURE 7. Individual PM force tracking responses of the adaptive training.

The reason for this can be the use of cables which connect PMs with the robot platform. More specifically, some jump points exist in FIGURE 7. This is surely caused by sudden human-robot interaction when the participant tried to change the trajectory. While these jump points can be easily filtered out, this study keeps them to support the presentation of the force distribution. Another interesting thing is the force tracking delay, as in Figs 6 and 7. The possible reason is the PMs' intrinsic compliance, where it takes a short time for the single-axis load cell (in joint space) to detect human-robot interaction (in task space).

V. DISCUSSION AND CONCLUSION

The joint-space controller, as a conventional scheme, is to make actual link lengths conform to desired lengths computed from the required manipulator posture [28]. An example is the control of the ankle robot by Jamwal, *et al.* [18]. By contrast, the task-space controller requires the orientation information of the robot end effector from a multi-DOF sensor or multiple sensors. Alternatively, forward kinematics that relies on numerical methods can be conducted to estimate robotic orientation. Noting that forward kinematics of a parallel robot manipulator has always been a challenging problem. In this robotic system, direct orientation measurement of the robot end effector was used to facilitate control feedback and inverse kinematics.

For rehabilitation training on a parallel mechanism, there is a higher accuracy requirement of robotic orientation compared with PMs' force tracking. Trajectory tracking is crucial to human users, while PMs' force tracking aims at 1) ensuring safety by preventing cables becoming loose; and 2) achieving maximum robot workspace by setting appropriate PM force. Noting that cascade control generally requires a good tuning of the inner loop performance. However, in this study, cables connecting PMs and robot platform made accurate force control highly difficult especially with real-time external disturbances from human users. Back to TABLE 1 and Figs 5, 7, while some jump points exist, this is acceptable since it meets the control requirement (all PMs in tension, and close to the force distribution trend). Again it is worth mentioning that this control method is specially design for cable-driven robotic device compared to those reported in [2], [3].

In addition to improved training safety of the cascade control, to achieve optimal benefits of robot-assisted rehabilitation, it is critical to promote active engagement from human users. Shahbazi, *et al.* [29] proposed an adaptive assist-as-needed control scheme to engage patients with the treatment process. Pehlivan, *et al.* [30] developed a trajectory generation algorithm based on an experimental movement profile, in which the trajectory was defined through piecewise polynomial functions. Regarding transitions between two different trajectories, Sanz-Merodio *et al.* [31] used a unitary Gaussian function to modulate it. However, this kind of trajectory recalculation method can increase online computational burden and tend to get a discontinuous desired speed and acceleration level. In contrast, the proposed trajectory adaptation strategy can be run in real time through detecting participants' movement intention from force sensors. The reference trajectory is defined based on a sinusoidal path where there is a low velocity at extreme ankle positions. Training safety can be further improved since trajectories reverse when an interaction force reaches the predefined threshold by changing its phase and frequency.

The proposed control strategy enables an adaptive training protocol. In early rehabilitation stage when the patient intends to be passive, the robot can be controlled for trajectory tracking using the cascade controller. After a training period when the patient has gained certain muscle strength, active mode can be carried out if an interaction force reaches the threshold, as described in FIGURE 3. The phase algorithm allows for adaptation of the movement direction, and the frequency adaptation helps to achieve adaptive movement velocity. By this algorithm, the robotic system can provide assistance when a participant has willingness to move but with inadequate actuation capacity. This helps to complete more exercises, and thus lead to enhanced clinical outcomes.

Some limitations still exist. First, the mechanical design of the ankle robot needs to be further improved, especially about robotic appearance. Second, the cables connecting PMs and the robotic moving platform are better replaced with universal joints, which will help to improve force tracking performance in joint space. Third, while the proposed control technique has been well validated with an ankle injured subject, more participants are needed to evaluate its reliability and clinical efficacy.

To summarize, contributions of this study mainly include: 1) proposing a cascade control scheme to ensure all PMs in tension for training safety, and optimal robot workspace with minimum energy consumption; and 2) proposing a movement intention-directed training algorithm that helps to enhance human-robot engagement and training safety. By using the proposed robot-assisted rehabilitation techniques, including using a parallel mechanism with appropriate workspace, cables controlled to be in tension, and an intention-directed training strategy, ankle therapy is expected to be safer and more effective.

REFERENCES

[1] H. I. Krebs, J. J. Palazzolo, L. Dipietro, M. Ferraro, J. Krol, K. Rannekleiv, B. T. Volpe, and N. Hogan, "Rehabilitation robotics: Performance-based progressive robot-assisted therapy," *Autonom. Robot.*, vol. 15, no. 1, pp. 7–20, Jul. 2003.

[2] Y. Pan, X. Li, and H. Yu, "Efficient PID tracking control of robotic manipulators driven by compliant actuators," *IEEE Trans. Control Syst. Technol.*, vol. 27, no. 2, pp. 915–922, Mar. 2019.

[3] Y. Fan, Z. Guo, and Y. Yin, "SEMG-based neuro-fuzzy controller for a parallel ankle exoskeleton with proprioception," *Int. J. Robot. Autom.*, vol. 26, no. 4, p. 450, 2011.

[4] M. Zhang, T. C. Davies, and S. Xie, "Effectiveness of robot-assisted therapy on ankle rehabilitation—A systematic review," *J. Neuroeng. Rehabil.*, vol. 10, p. 30, Mar. 2013.

[5] A. Roy, H. I. Krebs, D. J. Williams, C. T. Bever, L. W. Forrester, R. M. Macko, and N. Hogan, "Robot-aided neurorehabilitation: A novel robot for ankle rehabilitation," *IEEE Trans. Robot.*, vol. 25, no. 3, pp. 569–582, Jun. 2009.

[6] H. Yu, S. Huang, G. Chen, Y. Pan, and Z. Guo, "Human–robot interaction control of rehabilitation robots with series elastic actuators," *IEEE Trans. Robot.*, vol. 31, no. 5, pp. 1089–1100, Oct. 2015.

[7] G. Waldman, C.-Y. Yang, Y. Ren, L. Liu, X. Guo, R. L. Harvey, E. J. Roth, and L.-Q. Zhang, "Effects of robot-guided passive stretching and active movement training of ankle and mobility impairments in stroke," *Neurorehabilitation*, vol. 32, no. 3, pp. 625–634, 2013.

[8] M. Girone, G. Burdea, M. Bouzit, V. Popescu, and J. E. Deutsch, "A stewart platform-based system for ankle telerehabilitation," *Auton. Robots*, vol. 10, no. 2, pp. 203–212, Mar. 2001.

[9] J. E. Deutsch, J. Latonio, G. Burdea, and R. Boian, "Rehabilitation of musculoskeletal injuries using the Rutgers Ankle haptic interface: Three case reports," in *Proc. Eurohaptics*, Birmingham, U.K., 2001, pp. 11–16.

[10] J. Deutsch, J. Latonio, G. Burdea, and R. Boian, "Post-stroke rehabilitation with the Rutgers Ankle system: A case study," *Presence*, vol. 10, no. 4, pp. 416–430, Aug. 2001.

[11] D. Cioi, A. Kale, G. Burdea, J. Engsberg, W. Janes, and S. Ross, "Ankle control and strength training for children with cerebral palsy using the Rutgers Ankle CP: A case study," in *Proc. IEEE Int. Conf. Rehabil. Robot.*, Zürich, Switzerland, Jun./Jul. 2011, pp. 1–6.

[12] J. A. Saglia, N. G. Tsagarakis, J. S. Dai, and D. G. Caldwell, "A high-performance redundantly actuated parallel mechanism for ankle rehabilitation," *Int. J. Robot. Res.*, vol. 28, no. 9, pp. 1216–1227, 2009.

[13] J. A. Saglia, N. G. Tsagarakis, J. S. Dai, and D. G. Caldwell, "Control strategies for patient-assisted training using the ankle rehabilitation robot (ARBOT)," *IEEE/ASME Trans. Mechatronics*, vol. 18, no. 6, pp. 1799–1808, Dec. 2013.

[14] J. Yoon, J. Ryu, and K.-B. Lim, "Reconfigurable ankle rehabilitation robot for various exercises," *J. Robot. Syst.*, vol. 22, no. S1, pp. S15–S33, 2006.

[15] G. Liu, J. Gao, H. Yue, X. Zhang, and G. Lu, "Design and kinematics simulation of parallel robots for ankle rehabilitation," in *Proc. Int. Conf. Mechatronics Automat.*, Jun. 2006, pp. 1109–1113.

[16] C. E. Syrseloudis and I. Z. Emiris, "A parallel robot for ankle rehabilitation-evaluation and its design specifications," in *Proc. 8th IEEE Int. Conf. Bioinf. Bioeng.*, Athens, Greece, Oct. 2008, pp. 1–6.

[17] Y.-H. Tsoi, S. Q. Xie, and A. E. Graham, "Design, modeling and control of an ankle rehabilitation robot," in *Design and Control of Intelligent Robotic Systems* (Studies in Computational Intelligence), vol. 177. Berlin, Germany: Springer, 2009, pp. 377–399.

[18] P. K. Jamwal, S. Q. Xie, S. Hussain, and J. G. Parsons, "An adaptive wearable parallel robot for the treatment of ankle injuries," *IEEE/ASME Trans. Mechatronics*, vol. 19, no. 1, pp. 64–75, Feb. 2014.

[19] Q. Miao, M. Zhang, C. Wang, and H. Li, "Towards optimal platform-based robot design for ankle rehabilitation: The state of the art and future prospects," *J. Healthcare Eng.*, vol. 2018, Mar. 2018, Art. no. 1534247.

[20] M. Zhang, S. Q. Xie, X. Li, G. Zhu, W. Meng, X. Huang, and A. J. Veale, "Adaptive patient-cooperative control of a compliant ankle rehabilitation robot (CARR) with enhanced training safety," *IEEE Trans. Ind. Electron.*, vol. 65, no. 2, pp. 1398–1407, Feb. 2017.

[21] M. Hassan and A. Khajepour, "Analysis of bounded cable tensions in cable-actuated parallel manipulators," *IEEE Trans. Robot.*, vol. 27, no. 5, pp. 891–900, Oct. 2011.

[22] A. Campeau-Lecours, S. Foucault, T. Laliberte, B. Mayer-St-Onge, and C. Gosselin, "A cable-suspended intelligent crane assist device for the intuitive manipulation of large payloads," *IEEE/ASME Trans. Mechatronics*, vol. 21, no. 4, pp. 2073–2084, Aug. 2016.

[23] S. Xie, M. Zhang, and W. Meng, *Soft Robots for Healthcare Applications: Design, Modelling, and Control* (Healthcare Technologies), no. 14. London, U.K.: The Institution of Engineering and Technology, 2017.

[24] M. Zhang, J. Cao, G. Zhu, Q. Miao, X. Zeng, and S. Q. Xie, "Reconfigurable workspace and torque capacity of a compliant ankle rehabilitation robot (CARR)," *Robot. Auton. Syst.*, vol. 98, pp. 213–221, Dec. 2017.

[25] J. Sárosi, "New approximation algorithm for the force of fluidic muscles," in *Proc. 7th IEEE Int. Symp. Appl. Comput. Intell. Inform.*, Timisoara, Romania, May 2012, pp. 229–233.

[26] H. D. Taghirad and Y. B. Bedoustani, "An analytic-iterative redundancy resolution scheme for cable-driven redundant parallel manipulators," *IEEE Trans. Robot.*, vol. 27, no. 6, pp. 1137–1143, Dec. 2011.

[27] A. Pott, T. Bruckmann, and L. Mikelsons, "Closed-form force distribution for parallel wire robots," in *Computational Kinematics*, A. Kecskeméthy and A. Müller, Eds. Berlin, Germany: Springer, 2009, pp. 25–34.

[28] H. Guo, Y. Liu, G. Liu, and H. Li, "Cascade control of a hydraulically driven 6-DOF parallel robot manipulator based on a sliding mode," *Control Eng. Pract.*, vol. 16, no. 9, pp. 1055–1068, 2008.

[29] M. Shahbazi, S. F. Atashzar, M. Tavakoli, and R. V. Patel, "Robotics-assisted mirror rehabilitation therapy: A therapist-in-the-loop assist-as-needed architecture," *IEEE/ASME Trans. Mechatronics*, vol. 21, no. 4, pp. 1954–1965, Aug. 2016.

[30] A. U. Pehlivan, F. Sergi, and M. K. O'Malley, "A subject-adaptive controller for wrist robotic rehabilitation," *IEEE/ASME Trans. Mechatronics*, vol. 20, no. 3, pp. 1338–1350, Jun. 2015.

[31] D. Sanz-Merodio, M. Cestari, J. C. Arevalo, X. A. Carrillo, and E. Garcia, "Generation and control of adaptive gaits in lower-limb exoskeletons for motion assistance," *Adv. Robot.*, vol. 28, no. 5, pp. 329–338, Mar. 2014.

MINGMING ZHANG received the M.Eng. degree in mechatronics from Chongqing University, China, in 2012, and the Ph.D. degree in mechanical engineering from The University of Auckland, New Zealand, in 2015, where he has been a Research Fellow and/or Visiting Research Fellow with the Department of Mechanical Engineering, since 2015. In 2018, he joined the Southern University of Science and Technology, as an Assistant Professor. He has authored over 30 academic papers and one book. He holds over 20 patents. His research interests include mechatronics, medical robotics, biomechanics, computational modeling, and advanced control techniques. He has served as an Invited Reviewer for many high-quality international journals, including the IEEE TRANSACTIONS ON MECHATRONICS, the IEEE TRANSACTIONS ON BIOMEDICAL ENGINEERING, and the IEEE TRANSACTIONS ON INDUSTRIAL ELECTRONICS. He has also served as a Lead Guest Editor for the IEEE TRANSACTIONS ON AUTOMATION SCIENCE AND ENGINEERING and *Advances in Mechanical Engineering*.

ANDREW MCDAID received the B.E. (Hons.) and Ph.D. degrees from The University of Auckland, in 2008 and 2012, respectively. He is currently an Associate Professor with The University of Auckland, where he leads a large internationally recognized research group focusing on developing and translating novel medical devices to clinical and commercial uptake. Devices include robotics for rehabilitation (including exoskeletons and soft/smart materials), wearables, AI/ML data platforms, and neural prosthetics. He has published more than 60 research papers and holds three provisional patents. His main research interests include design and control of medical devices, functional electrical stimulation of neuroprosthetics, smart materials, soft robotics, physiological control (EEG, HD-EMG), gamification, and developing intelligent medical robotics for people who have suffered injury, stroke or have disabilities.

ALLAN J. VEALE received the B.E. degree (Hons.) in mechatronics engineering and the Ph.D. degree from The University of Auckland, New Zealand, in 2013 and 2017, respectively. His thesis focused on the development of a wearable fluidic actuator with embedded sensors for rehabilitation devices along with related modeling tools.

During this research, he published four journal articles and three conference papers. He is currently a Postdoctoral Fellow with the University of Twente, The Netherlands, where he also works on high-power soft and wearable actuation systems. In addition to these clothing-like, inflatable structures, he also has background in the fabrication, testing and modeling of dielectric elastomer sensors, and research interests in user-centered medical devices and novel wearable energy sources. These research topics underpin Allan's aim to explore the extent and manner that active, soft, and clothing-like structures can mechanically assist human movement. He envisions such structures empowering people with health and mobility impairments to engage fully in society, in first or third world countries.

YUXIN PENG received the bachelor's and master's degrees from Chongqing University, China, in 2007 and 2010, respectively, and the Ph.D. degree from the Department of Nanomechanics, Tohoku University, Japan, in 2013. He was a Research Fellow with the Department of Biomedical Engineering, National University of Singapore, Singapore, from 2014 to 2016. He is currently a Professor with the Department of Physical Education and Sports Science, Zhejiang University, China. His research interests include smart sensors, actuators, and biomechanics. He has authored over 40 academic papers and served as an Invited Reviewer for many high-quality international journals, including the IEEE TRANSACTIONS ON MECHATRONICS, *Sensors and ActuatorsA: Physical*, *Review of Scientific Instruments*, *Applied Sciences*, *Microsystem Technologies*, and *Chinese Journal of Mechanical Engineering*.

SHENG QUAN XIE received the M.E. and Ph.D. degrees in mechatronics from the Huazhong University of Science and Technology, Wuhan, China, in 1995 and 1998, respectively, and the Ph.D. degree in manufacturing automation from the University of Canterbury, Canterbury, New Zealand, in 2002. From 2003 to 2016, he was with The University of Auckland, as a Chair Professor. Since 2017, he joined the University of Leeds, where he is currently a Chair Professor in the area of biomechatronics. He has published two books, 15 book chapters, and over 200 international journals and conference papers. His current research interests include smart sensors and actuators, medical and rehabilitation robots, microelectromechanical systems, modern control technologies and applications, and rapid product development technologies, methods, and tools. He is an Editor-in-Chief for the *International Journal of Biomechatronics and Biomedical Robotics* and an Associate Editor for the *International Journal of Advanced Mechatronic Systems* and the *International Journal of Mechatronics and Intelligent Manufacturing*.